

Design of Sub-90 nm Low-Power and Variation Tolerant PD/SOI SRAM Cell Based on Dynamic Stability Metrics

Rajiv V. Joshi, *Fellow, IEEE*, Saibal Mukhopadhyay, *Member, IEEE*, Donald W. Plass, Yuen H. Chan, Ching-Te Chuang, *Fellow, IEEE*, and Yue Tan

Abstract—In this paper we have studied the impacts of floating body effect, device leakage, and gate oxide tunneling leakage on the read and write-ability of a PD/SOI CMOS SRAM cell under V_t , L and W variations in sub-100 nm technology for the first time. The floating body effect is shown to degrade the read stability while improving the write-ability. On the other hand, the gate-to-body tunneling current improves the read stability while degrading the write-ability. It is also shown that the use of high- V_t and thick oxide cell transistors can improve leakage, read and write-ability without causing significant performance degradation. The test-chip is fabricated in sub-90 nm SOI technology to show the effectiveness of high- V_t and thick-oxide devices in improving stability of SRAM cells.

Index Terms—Dynamic stability, high- V_t , process variation, SRAM, thick oxide, write-ability.

I. INTRODUCTION

WITH technology scaling, inter-die and intra-die variations in process parameters (channel length (L), width (W), threshold voltage (V_t) etc) have become serious problems in circuit design [1], [2]. The device-to-device (intra-die) variations in L , W or V_t between the neighboring transistors in an SRAM cell can significantly degrade the stability of the cell. The static stability of a cell is measured by the static noise margin (SNM) [3]. In [3] authors have analyzed the impact of device-to-device V_t fluctuations on the SNM of a bulk CMOS SRAM cell. However, in a PD/SOI SRAM cell, due to the floating body effect, the strength of the different transistors in the cell varies during read and write operations [4]. Even if the static stability of the cell is high, device-to-device fluctuations may result in instability during the read and write operations. In addition, the initial states of cell transistors as well as gate-to-body tunneling current are very critical in cell stability. Hence, a thor-

ough understanding of the dynamic stability under parameter variations is crucial to maintain/exploit the performance advantage of PD/SOI technology. We have also analyzed the impact of using high V_t and thick oxide transistors on the performance and stability of the cell. It has been observed that, use of high V_t and thick oxide cell transistors can significantly reduce the cell leakage, improve the cell stability without causing significant performance degradation. Notice that in this study, parameters are treated as independent and variations are applied in the worst case directions, thus representing the worst case scenario. Test-chip is fabricated in sub-90 nm PD/SOI technology and measured to demonstrate the effectiveness of the high- V_t and thick-oxide devices. The measurement results verifies the simulation based predictions and demonstrate that, use of higher- V_t and thicker-oxide devices can significantly improve the cell stability and hence, SRAM yield.

II. DYNAMIC CELL STABILITY

In this section, we present the concept and the methods for analyzing dynamic stability of SRAM cell.

A. Dynamic Stability

The strengths of the PMOS and NMOS transistors in an SRAM cell (Fig. 1) control the read stability and write-ability (collectively known as cell stability) of the SRAM cell. The strength is defined by the threshold voltage (V_t), channel length (L), and channel width (W) of transistors. The conventional static stability analysis focuses on the beta ratio (which is determined by the L and W ratios) and V_t s of pass-gates and cross-coupled PFET/NFET. The V_t used in such analysis is normally the V_t measured at a particular terminal (i.e., V_{ds} and V_{gs}) voltages (e.g., at $V_{ds}-V_{DD}$). However, due to short channel effects, such as Drain Induced Barrier Lowering (DIBL), the V_t of a device depends on its terminal voltages and hence, changes dynamically for different voltages at cell terminals (e.g., wordline, bitlines, cell supply) as well as cell nodes (i.e., V_{DD} or 0 at a given node) [9]. Further, for PD/SOI devices, the operating conditions (i.e., V_{ds} and V_{gs} values) of a device also modify the threshold voltage due to floating body effect. Moreover, the read/write operation of a cell also depends on the capacitances at the cell nodes, which can only be captured through transient analysis. Therefore, for a true analysis of the cell stability, static analysis considering parameters such as L , W , and V_t , as well as transient analysis considering dynamic changes in the bias conditions and corresponding effects

Manuscript received May 04, 2008; revised December 03, 2008. Current version published February 25, 2009.

R. V. Joshi is with the IBM T. J. Watson Research Center, Yorktown Heights, NY 10598 USA (e-mail: rvjoshi@us.ibm.com).

S. Mukhopadhyay is with the School of Electrical and Computer Engineering, Georgia Institute of Technology, Atlanta, GA (e-mail: saibal@ece.gatech.edu).

D. W. Plass and Y. H. Chan are with IBM Poughkeepsie, NY 12601-5400 USA (e-mail: plassd@us.ibm.com; chany@us.ibm.com).

C. T. Chuang is with the National Chiao Tung University, Hsinchu, Taiwan (e-mail: chingte.chuang@gmail.com).

Y. Tan is with IBM Fishkill, Hopewell Junction, NY 12533-6683 USA (e-mail: yuetan@us.ibm.com).

Color versions of one or more of the figures in this paper are available online at <http://ieeexplore.ieee.org>.

Digital Object Identifier 10.1109/JSSC.2009.2013768

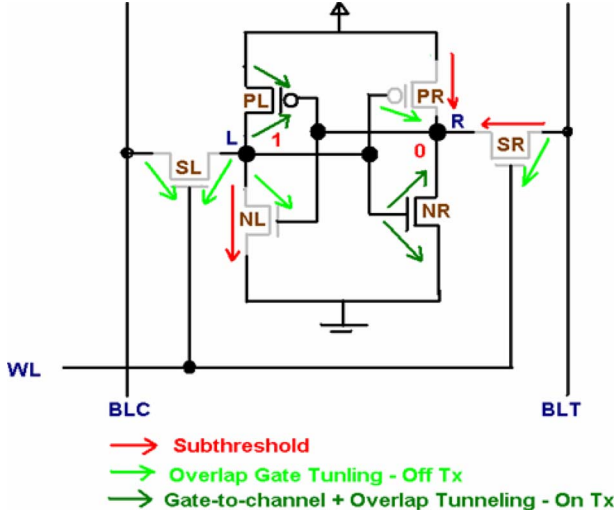


Fig. 1. A SRAM cell storing “1”.

in device parameters need to be considered. The ‘dynamic stability analysis’ evaluates cell stability considering both the static and bias-dependent transient effects, and hence provides a more accurate measure of stability of SRAM cell in operation. In dynamic analysis instead of performing a DC analysis of SRAM cell, a transient analysis is performed considering dynamic voltage waveforms at wordline and bitlines. In a true sense dynamic stability can be defined as the critical noise level required in the cell to prevent the upset or corruption under dynamically stressing the transistors. In this work, for read stability or write-ability analysis considering random V_t mismatch, we consider the ‘noise’ as the worst case V_{th} variation (the read and write operations have different worst case conditions as explained in following sections). To estimate dynamic stability for read or write operations, we first apply certain worst-case V_{th} mismatch. Next, we consider different V_{DD} values defining cell, bitline, and wordline voltage levels, and perform transient analysis for read or write operations. In the transient analysis wordline slew rate is varied from low to high to explore the worst case condition for the cell. The SRAM cell as well as the peripherals is considered in the analysis to obtain a comprehensive picture. The effect of array organization, such as the impact of other cells on the same column and/or same row, is also considered. The considerations of array organization and peripherals provide a more accurate measure of stability compared to static/DC analysis (such as Static Noise Margin for read stability) which considers ‘a cell in isolation’. The transient simulations (with standard waveforms for read/write operations) provide an indication of correct (stable) or faulty (unstable) operation of the cell at a given V_{DD} level. The range of V_{DD} which provides correct (stable) operations is used as an indicator of the dynamic read stability or write-ability. Note, that V_{DD} level is just one option, one can also perform dynamic stability analysis by modifying the operating frequency, wordline pulse width, etc.

In summary, the dynamic stability of the cell is a measure of the robustness of the cell against parameter variations during the read (read stability) and write (write stability, or “write-ability”) operation. The dynamic stability measures the ac characteristics

of the cell and provides more detail information regarding the cell functionality compared to the static noise margin. Since dynamic stability captures the cell behavior in the ac mode (e.g., frequency response of the cell, the effect of node capacitances, floating body effect in SOI as discussed later) it is a better indicator of the actual product behavior.

In the following sections, we discuss the dynamic stability analysis for read and write operation in an SRAM cell. In this analysis, sub-90nm PD/SOI SRAM cell is used. Further, the analysis consider a PD/SOI SRAM cell which stores ‘1’ (i.e., $V_L = '1'$ and $V_R = '0'$) (Fig. 1). The analysis is same for a cell storing ‘0’ (i.e., $V_L = '0'$ and $V_R = '1'$), which is not repeated for brevity. To explain the effects of V_t variation on read stability and write-ability we have used simplified equations considering square-law transistor model. However, the results are obtained using circuit simulations for the sub-90nm PD/SOI cell.

B. Read Stability

During the read operation, the access transistor S_R and the NMOS transistor N_R form a resistor-voltage-divider between node BLT and node R . This increases V_R to an intermediate voltage (V_{READ}) which subsequently increases the sub-threshold leakage through N_L , thereby discharging V_L from ‘1’. A reduction in V_L further reduces the strength of N_R (since $V_{gs}(N_R) = V_L < V_{DD}$) and hence cause V_R to rise more [5], [7]. If V_{READ} is higher than the trip point of the inverter P_L - N_L , the state of the cell gets flipped (i.e., $V_L = '0'$ and $V_R = '1'$ after reading). This is known as ‘destructive read’ or ‘unstable read’. A simple static condition for read stability can be defined as [7], [8]:

$$V_{TRIP}(P_L - N_L) > V_{READ}. \quad (1)$$

The intermediate voltage can be obtained by solving V_{READ} :

$$\begin{aligned} I_{ds}(S_R)(V_{DD} - V_{READ}, V_{DD} - V_{READ}) \\ + I_{ds}(P_R)(V_L - V_{DD}, V_{READ} - V_{DD}) \\ = I_{ds}(N_R)(V_L \approx V_{DD}, V_{READ}) \end{aligned} \quad (2)$$

where, I_{ds} (gate-source, drain-source) represents the drain-to-source current. For the sake of simplicity, in the above formulation we have neglected the gate leakage contributions to node R .

1) *Worst-Case Condition for Read-Stability*: From (1) we can observe that, if the relative strength of P_R and S_R increases while that of N_R reduces, V_{READ} increases thereby increasing the possibilities of the read failure. Hence, the worst-case for read stability occurs if due to process variation, S_R and P_R becomes strong (V_t & L reduces, W increases) whereas N_R becomes weak (V_t & L increases, W reduces).

2) *Impact of Floating Body Effect in PD/SOI*: In PD/SOI various effects such as gate-to-body coupling (which causes kink effect), drain-to-body, body-to-source coupling can affect the body voltages. In PD/SOI SRAM before the start of the read operation, the V_{ds} of S_R is V_{DD} which increases the body-voltage of S_R . The body-voltage of N_R is much lower as $V_{ds}[V_{BODY}(N_R) = 0]$. This is evident from the waveform shown in Fig. 2 which shows the body voltage of different transistors before and during read operations. Further, since node L is at ‘1’, body voltage of both N_R and P_R are also higher. Since a higher

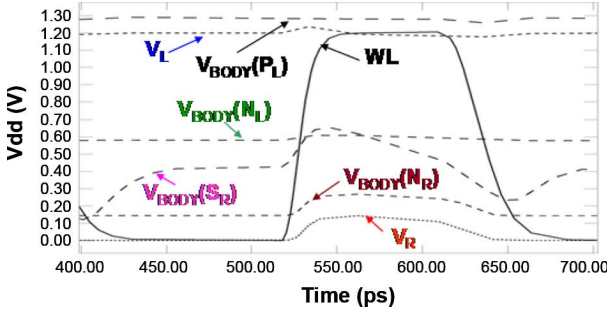


Fig. 2. Waveform for read operation showing body voltage of different transistors.

body voltage for NMOS indicates a stronger device (i.e., lower V_{th}) while a higher body voltage for PMOS indicates a weaker device (i.e., higher V_{th}), the floating body effect results in (1) stronger S_R and weaker N_R (higher V_{READ}); and (2) stronger N_L and weaker P_L [lower V_{TRIP} ($P_L - N_L$)]. Therefore, floating body-effect tends to marginally degrade the read stability.

3) *Impact of Leakage on Read Stability:* The high leakage in the nano-scaled transistors plays an important role in determining the read-stability. A larger subthreshold leakage of the transistor N_L reduces the voltage V_L during read operation and thereby affects read-stability. A larger subthreshold leakage of P_R also negatively affects read stability by increasing V_{READ} . Also in the presence of large number of cells on the same bit column having opposite state as that of the selected cell can increase leakage on bitlines which slows down the bit-line discharge. Due to back to back body diodes in PD SOI (reverse diode from drain to body and forward diode from body to source) the other leakage component (parasitic bipolar current) exists from drain-to-body-to-source. This has a similar effect on the cell stability as that of sub-threshold leakages. A slower bit-line discharge indicates a higher V_{ds} stress for S_R thereby affecting read stability. Similarly, as shown in Fig. 1, the gate-to-channel and the overlap tunneling leakage from the transistors N_R , N_L , P_R and P_L entering into the node R, cause V_R to rise more during read operation and hence degrade the read stability. While the gate-to-body tunneling leakage is much smaller than the other leakage components, it has interesting implications for PD/SOI SRAM cell. For PD/SOI devices, however, the gate-to-body tunneling current charges/discharges the floating body, thus changing the body voltage and V_t . When the gate of a transistor at “VDD” and source and drain are at “0”, initially the body sits at “0”. The gate-to-body tunneling current charges the transistor body. Similarly, when gate is at ‘0’ the gate-to-body tunneling current tends to discharge the body-voltage. Therefore, gate-to-body tunneling current reduces the body-voltage of S_R and N_L (gate at V_{DD}) thereby weakening them. It also reduces body-voltage of P_L which makes it stronger. On the other hand, gate-to-body tunneling increases the body-voltage of N_R (gate at V_{DD}) thereby making it stronger [6]. This helps to reduce V_{READ} (stronger N_R and weaker S_R) and increase V_{TRIP} (stronger P_L and weaker N_L), thereby improving read stability. Hence, the presence of gate-to-body tunneling current helps to improve the read stability of PD/SOI SRAM cell.

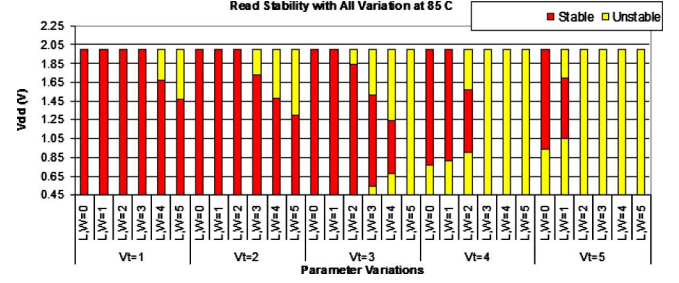


Fig. 3. Variation of read-stability at $T = 85^\circ\text{C}$ for different L , W and V_t variation (normalized unit for variation) .

4) *Circuit Simulation Results for Read Stability:* To measure the read stability, we have applied the V_t , L and W variations in the worst-case direction and varied the V_{DD} from a low to a high value. We have measured the V_{DD} region in which the cell is stable for each unit of variation in V_t , L and W . A larger stable region indicates a better robustness against read failure due to process variation. Fig. 3 shows the read stability of the cell at $T = 85^\circ\text{C}$ with application of different parameter variation. Note, that the figure shows two different unstable regions. This is due to the counter-acting effects of V_{DD} on the cell characteristics. As mentioned earlier, in this simulation, we consider same V_{DD} value for cell supply, wordline voltage, and bitline voltage. A lower wordline V_{DD} implies a lower gate voltage for the pass-gates and a lower bitline V_{DD} implies a lower V_{ds} stress across the pass-gate. Both of these reduces the pass-gate strength and helps to reduce V_{READ} . However, a lower cell V_{DD} reduces the trip-point and the strength of the pull-down device (N_R) in the read path. Both of these negatively impact the read stability. At very low voltage, the negative effect of lower cell V_{DD} results in unstable read operations. On the other hand, at very high V_{DD} , the increased strength of the access device results in unstable read. Note, that during read operation the pass-gate S_R is in saturation while N_R is in linear. Since saturation current is a stronger function of V_{GS} (e.g., quadratic) compared to linear current, a higher wordline V_{DD} increases V_{READ} resulting in unstable read operation. This explains the origin of two unstable regions related to read operations. Further, a higher V_{DD} also increases the V_{th} mismatch between S_R and N_R due to DIBL effect [as V_{ds} for S_R ($= V_{DD} - V_{READ}$) $>$ V_{ds} for N_R (V_{READ}) \Rightarrow due to DIBL $V_t(S_R) < V_t(N_R)$] which negatively impacts read stability [9]. Moreover, as explained in the following section, for PD/SOI the floating body effect results in a lower V_{th} for S_R from N_R at the start of read operation. At a higher V_{DD} the body-voltage difference between S_R and N_R is higher which also degrades read stability. It can be observed that, the impact of V_t variation is very significant. The impact of the L & W variation becomes significant when coupled with V_t variation. The stronger effect of V_{th} variation originates from the stronger-than-linear dependence of saturation current on V_t which results in a stronger sensitivity of V_{READ} and V_{TRIP} to V_t compared to L and W (both linear and saturation current depends linearly on L and W). Considering a given V_t variation and different amount of L and W variation it was observed that, read stability marginally degrades at a higher

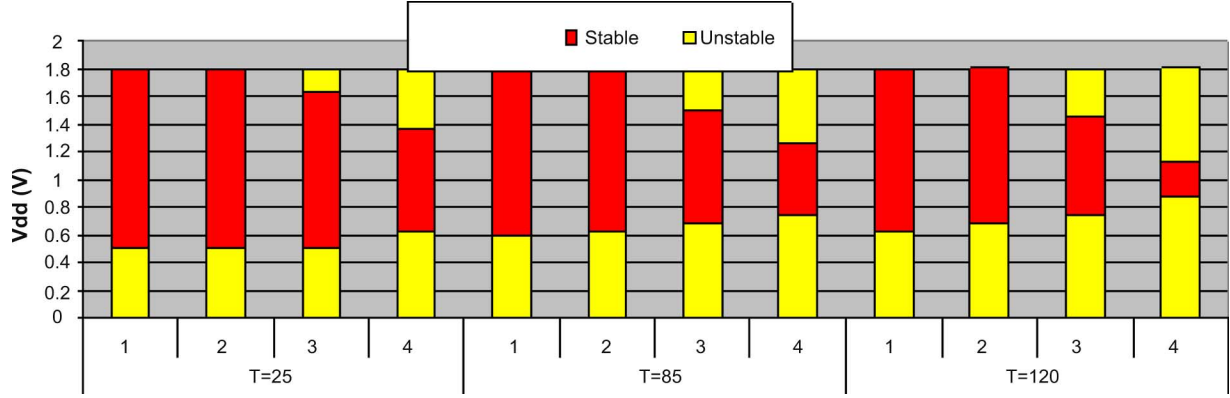


Fig. 4. Effect of temperature on read stability: L and W variation along with V_t variation of 3 unit.

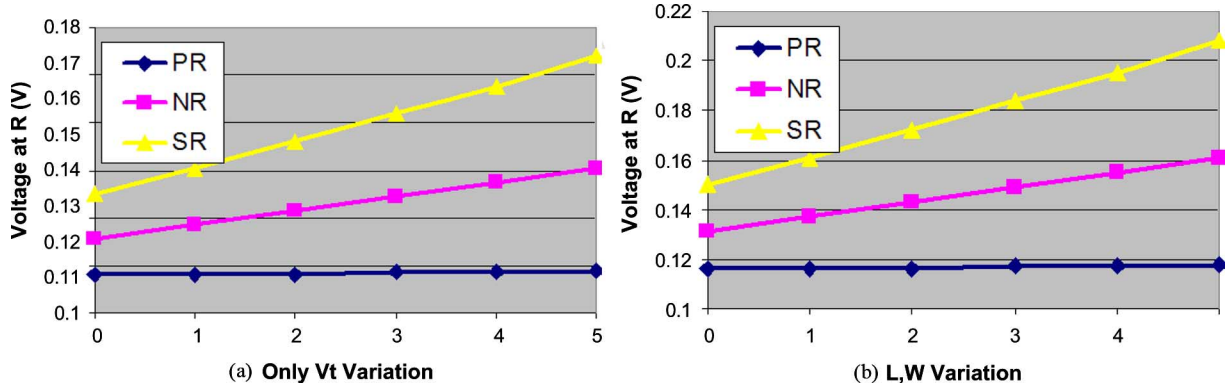


Fig. 5. Impact of variation of different transistor on the read stability. (a) V_t variation (b) L, W variation (with 3 units of V_t variation). A higher voltage at node R indicates a worse read-stability (normalized unit for variation).

temperature (Fig. 4). This is mainly because; at a higher temperature mobility degrades. Further, linear current depends more strongly on mobility compared to saturation current (velocity saturation effect in short-channel devices makes saturation current less sensitive to mobility). Hence, at a higher temperature due to lower mobility, linear current reduces more than saturation current resulting in a higher V_{READ} and degraded read stability. The temperature sensitivity increases if L & W variation increases as sensitivity of β -ratio [where, $\beta = \mu_{\text{eff}} C_{\text{ox}}(W/L)$] to L, W mismatch depends on mobility which in turn depends on mobility. At a higher temperature, the leakage current contributed by P_R [see (2)] increases. This leakage contribution also increases when L mismatch is considered (as worst-case L mismatch means lower L for P_R). The higher temperature coupled with V_t and L mismatch can significantly increase the leakage current contribution resulting in a higher V_{READ} and lower read stability. Fig. 5 shows V_{READ} at different V_t , L and W variation, by applying the variations to transistors S_R , N_R and P_R one at a time. It can be observed that, application of variation in S_R cause maximum rise in V_{READ} . This indicates that S_R is most critical for read stability. This is because of the stronger-than-linear dependence of saturation current of S_R on device V_{th} . The impact of P_R is minimum since it is in the subthreshold region. From Fig. 4, it can be concluded that to optimize the cell for best read stability we need a weak access transistor while a strong pull-down NMOS. The effect of gate-to-body tunneling current on the read stability is

shown in Fig. 6. It can be clearly observed that, the presence of gate-to-body tunneling current improves the read stability of PD/SOI SRAM cell.

C. Write-Ability

While writing a '0' to the cell shown in Fig. 1 (i.e., changing the state of the cell from ($V_L = '1'$ and $V_R = '0'$) to ($V_L = '0'$ and $V_R = '1'$)), the low going bit-line BLC forms a voltage divider between the PMOS P_L and the access transistor S_L . If due to this voltage division the voltage at node L (V_{WRITE}) is reduced below the trip point of the inverter P_R - N_R within the time-interval when WL is high (T_{WL}) then a successful write occurs [4]–[8]. Hence, the stability conditions for write operations can be formulated as [5], [7], [8]:

$$T_{\text{WRITE}} < T_{\text{WL}} \quad (3)$$

where T_{WRITE} is the time required to reduce the voltage V_L from V_{DD} to the trip-point of P_R - N_R . T_{WRITE} can be obtained by:

$$T_{\text{WRITE}} = \int_{V_{\text{TRIP}}(P_R-N_R)}^{V_{\text{DD}}} \frac{C_L}{I_{\text{ds}}(S_L) + I_{\text{ds}}(N_L) - I_{\text{ds}}(P_L)} dV_L \quad (4)$$

Note, a stronger P_L and weaker S_L increases write time and degrades write-ability.

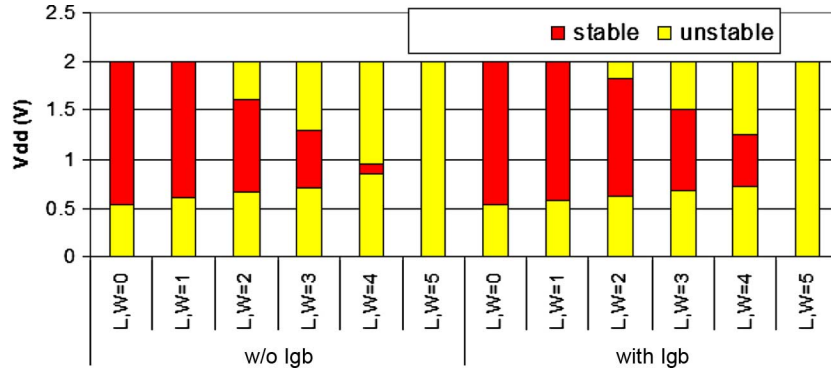


Fig. 6. Impact of gate-to-body tunneling current on read-stability (normalized unit for variation).

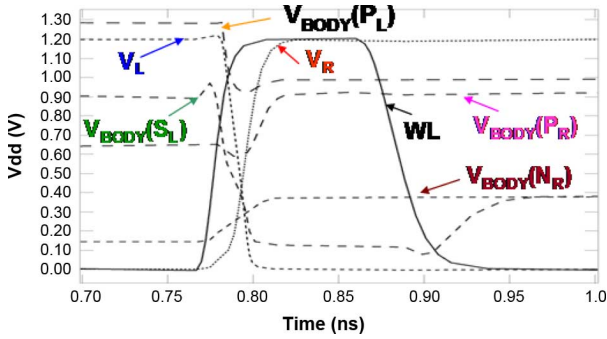


Fig. 7. Waveform showing body voltages during write operation.

1) *Worst-Case Condition for Write-Ability*: From (3)–(4) we can observe that, if the relative strength of P_L increases while that of S_L and N_L reduces the net discharging current for node ‘L’ [$= I_{ds}(S_L) + I_{ds}(N_L) - I_{ds}(P_L)$] becomes lower thereby increasing T_{WRITE} . Further, a weaker S_R and P_R and a stronger N_R reduce the trip-point of P_R - N_R which also increases T_{WRITE} . Hence, the worst-case condition for write-ability occurs if due to process variation, (a) P_L becomes strong (V_t and L reduces, W increases) whereas S_L and N_L become weak (V_t & L increases, W reduces) resulting in lower discharging current; and (b) S_R and P_R become weak (higher V_t & L , lower W) and N_R becomes strong (lower V_t and L , higher W) resulting in lower trip-point of P_R - N_R .

2) *Impact of Floating Body Effect in PD/SOI*: In PD/SOI SRAM before the start of the write operation, body voltage of S_L [$V_{BODY}(S_L)$] and P_L [$V_{BODY}(P_L)$] are high (since drain and source at V_{DD}). This is shown Fig. 7 which shows the body-voltages of different transistors before and during a typical write operation. This results in a stronger S_L and weaker P_L and thus improves the write-ability. Further, since node R is at ‘0’, $V_{BODY}(N_R)$ is low ($V_{drain} = V_{source} = 0$) while $V_{BODY}(S_R)$ is high ($V_{ds} \sim V_{DD}$), resulting in a weaker N_R and stronger S_R . The body voltage of P_R is also less (as $V_{drain} = 0$) resulting in a stronger P_R . Stronger S_R and P_R and weaker N_R improves write-ability. Therefore, floating body effect tends to improve the write-ability.

3) *Impact of Leakage on Write-Ability*: A large subthreshold leakage of the transistor N_L helps to discharge V_L . The gate-to-channel and overlap-tunneling leakage of the transistors N_R , N_L , P_R and P_L also helps to discharge V_L and

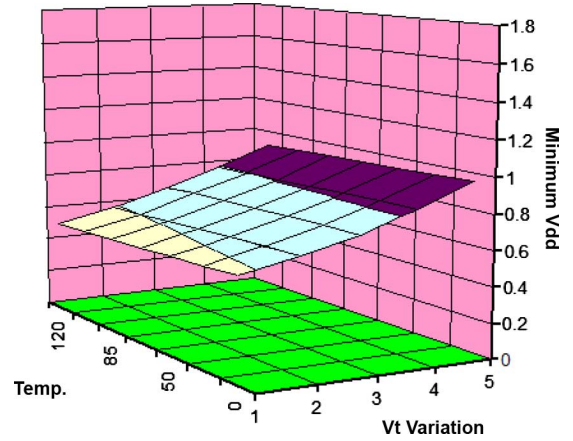


Fig. 8. Write-ability at with V_t and Temperature variation.

hence improves write-ability. On the other hand, gate-to-body tunneling reduces the body voltages of N_L , S_L , S_R , P_L (gate at ‘0’). This weakens N_L , S_L , and S_R while strengthens P_L thereby degrading write-ability [5]. For the worst case write operation all the unselected cells have same polarity as that of the selected cell. When the node holding “1” needs to be written to “0”, parasitic bipolar currents induced in pass gates can reduce the currents to discharge the bitline degrading the “write-ability”. Similarly, gate-to-body tunneling increases body voltages of N_R (makes it stronger) and P_R (makes it weaker) as both of them have gate at V_{DD} . This lowers the V_{TRIP} of (P_R - N_R). Therefore, gate-to-body tunneling current degrades the write-ability of PD/SOI SRAM cell. It is interesting to note that, for PD/SOI devices floating body effect degrades read stability while improves write-ability. On the other hand, gate-to-body tunneling improves read stability while degrades write-ability.

4) *Circuit Simulation Results for Write-Ability*: To measure the write-ability, we have applied the V_t , L and W variations in the worst-case direction and varied the V_{DD} from a low to a high value. As V_{DD} increases, the strength of S_L increases, thereby increasing the write-ability. We have measured the minimum V_{DD} (V_{DDmin}) at which the cell remains writable. A lower value of V_{DDmin} indicates a better write-ability. Fig. 8 shows the variation of the V_{DDmin} with application of only V_t variation at different temperature. It can be observed that,

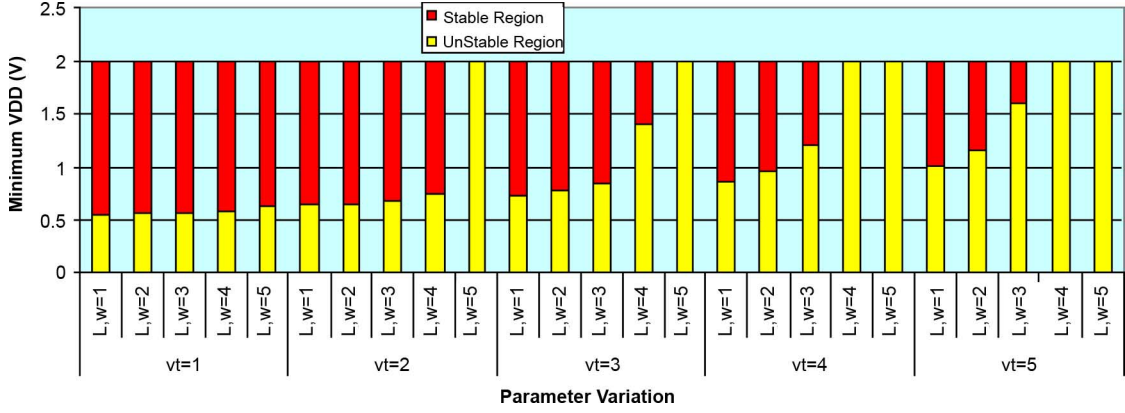


Fig. 9. Write-ability with all variation at $T = 85^\circ\text{C}$ (normalized unit for variation).

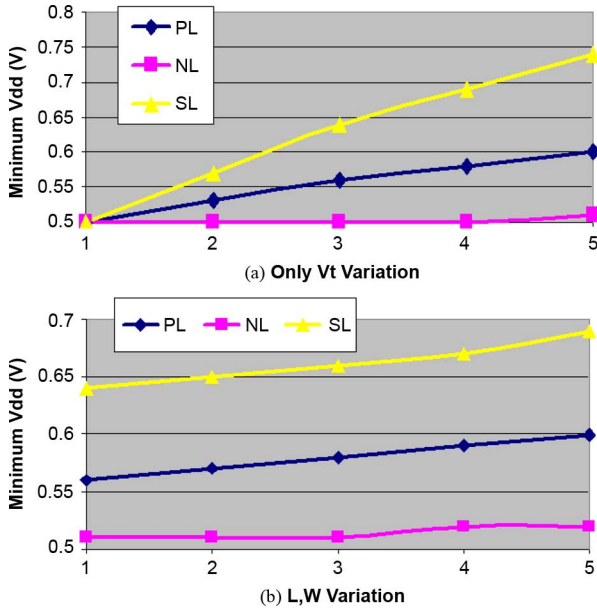


Fig. 10. Impact of variation of different transistor on the write-ability. (a) Vt variation (b) L, W variation. A lower $V_{DD\min}$ indicates better write-stability (normalized unit for variation).

$V_{DD\min} > V_{DD} (= 0.9\text{ V})$ if Vt variation is high. It can also be observed that, the sensitivity with temperature is not very high. The sensitivity of the $V_{DD\min}$ with respect to L and W variation alone is very low (figure not shown). However, if L and W variation is coupled with Vt variation, it has a strong impact (Fig. 9). The effect of temperature variation was observed to be small. Fig. 9 shows $V_{DD\min}$ with application of Vt (Fig. 10(a)) and $\langle L \text{ and } W \rangle$ (Fig. 10(b)) variations to transistors S_L , P_L and N_L alone. It can be observed that, the access transistor S_L is most critical whereas N_L has little impact (since it is in subthreshold region). Hence, a weaker PMOS pull-up and a stronger NMOS access transistor are required for better write-ability.

III. STABILITY WITH HIGH-VT TRANSISTORS

In order to reduce the subthreshold leakage in the cell, scaled SRAM cells are often designed with high Vt transistors. It has been observed that the performance degradation associated with

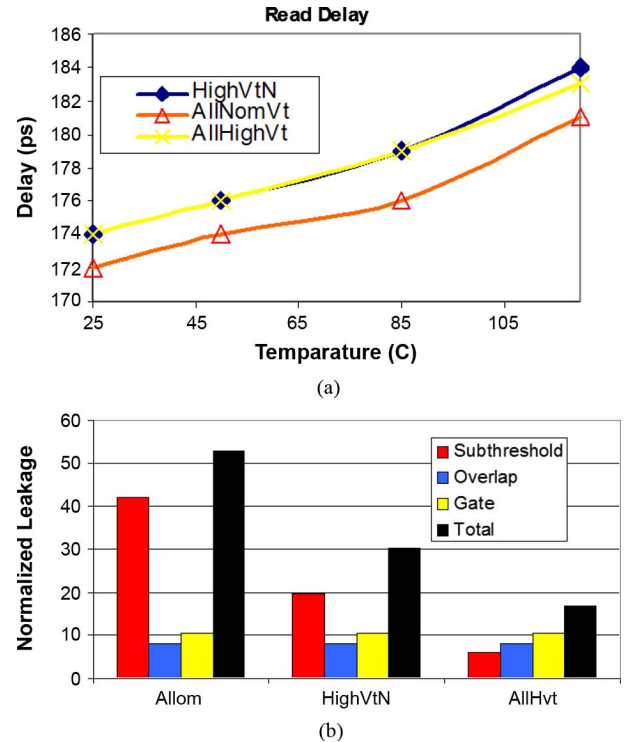


Fig. 11. Impact of using high Vt transistor on the performance and leakage of an SRAM cell: (a) Read delay vs. temperature, (b) Leakage components in stand-by mode. Notice that, significant leakage reduction is possible with small performance degradation by using high Vt transistors.

the use of high Vt transistors are not very significant. Fig. 11 shows the read delay (Fig. 11(a)) and the leakage (Fig. 11(b)) of the SRAM cell designed with all nominal Vt (*AllNomVT*), high Vt NMOS (*HighVtN*) and all high Vt transistors (*AllHVT*). It can be observed that, leakage improves significantly from *AllNomVT* to *AllHVT* ($> 4\times$) and the associated performance degradation is quite small ($< 2\%$). The subthreshold leakage shows maximum reduction with higher-Vt transistors. The leakage reduction obtained with high-Vt increases at a higher temperature as the current contribution from the subthreshold leakage is much higher. In the following sections we will describe the impact of using high-Vt transistors on the stability of the cell.

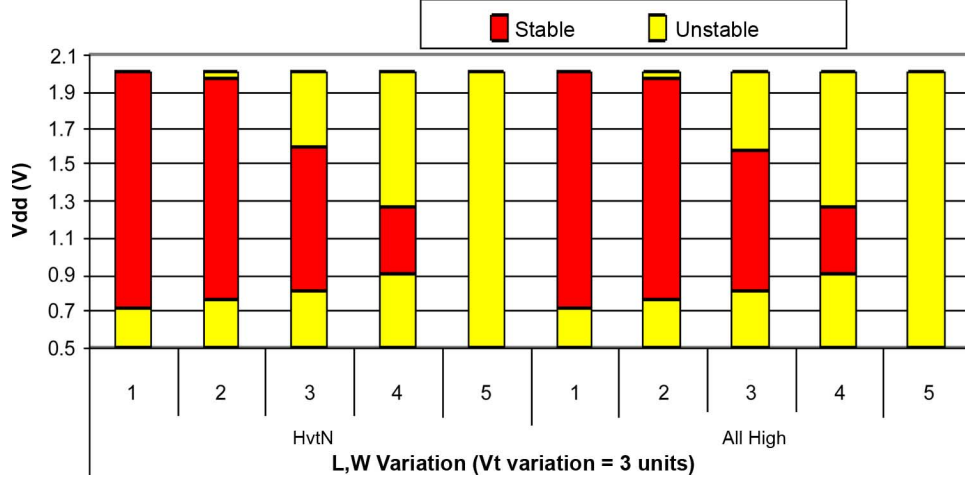


Fig. 12. Impact of using High Vt transistors on read-stability. X axis represents normalized units of L, W variations along with 3 units of Vt variations.

A. Read Stability With High Vt

In order to analyze the impact of high Vt transistors, let us assume a simplified square-law transistor characteristics. Under this assumption, the trip point of the inverter P_L-N_L can be given by

$$V_{TRIP} = \frac{V_{DD} - V_{tp0} - \Delta V_{tp} + (V_{tn0} + \Delta V_{tn}) \sqrt{\left(\frac{\beta_{NL}}{\beta_{PL}}\right)}}{1 + \sqrt{\left(\frac{\beta_{NL}}{\beta_{PL}}\right)}}$$

or

$$V_{TRIP} = V_{TRIP0} + \frac{\Delta V_{tn} \sqrt{\left(\frac{\beta_{NL}}{\beta_{PL}}\right)} - \Delta V_{tp}}{1 + \sqrt{\left(\frac{\beta_{NL}}{\beta_{PL}}\right)}} \quad (5)$$

where β for each transistor is given by

$$\beta = \left(\frac{\mu_{eff}\epsilon}{T_{ox}}\right) \left(\frac{W}{L}\right) \quad (6)$$

V_{tp0} and V_{tn0} represents the nominal PMOS and NMOS Vt, V_{TRIP0} represents the trip point with nominal Vt and ΔV_{tp} and ΔV_{tn} represents the difference between high and nominal Vt. From (6) it can be observed that, use of higher Vt for NMOS increases the trip point whereas increasing the PMOS Vt lowers the trip point. Since in SRAM $\beta_{NL} > \beta_{PL}$ (because $(W/L)_{PMOS} < (W/L)_{NMOS}$ and $\mu_P < \mu_N$), increasing Vt of NMOS has a stronger impact (assuming $\Delta V_{tp} \approx \Delta V_{tn}$) on the trip point of the inverter. Similarly, V_{READ} can be given by (assuming $V_{tn_{SR}} \approx V_{tn_{NR}} = V_{tn}$) [5]:

$$V_{READ} = \frac{(V_{DD} - V_{tn0} - \Delta V_{tn}) \left(1 + \sqrt{\left(\frac{\beta_{NR}}{\beta_{SR}}\right)} \pm \sqrt{\left(\frac{\beta_{NR}}{\beta_{SR}}\right) + \left(\frac{\beta_{NR}}{\beta_{SR}}\right)}\right)}{1 + \sqrt{\left(\frac{\beta_{NR}}{\beta_{SR}}\right)}} \quad (7)$$

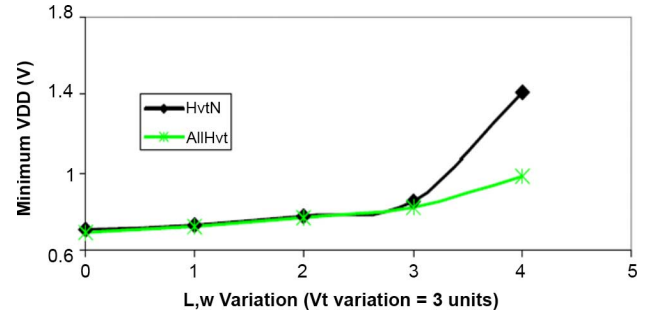


Fig. 13. Impact of using high Vt transistors on write-ability. X-axis represents different units of L, W variation along with 3 units of Vt variation.

The use of high Vt NMOS N_R increases the on resistance of the pull-down path and thus results in a higher V_{READ} . However, high Vt NMOS S_R lowers the current into the node R and hence lowers V_{READ} . It can be observed from Fig. 5 that S_R is more critical than N_R in increasing V_{READ} due to parameter variation. Hence, using high Vt NMOS decreases the V_{READ} (see (7)) and helps to improve read-stability. Simultaneously, high Vt NMOS increases the trip point of the inverter P_L-N_L and reduces the subthreshold leakage of N_L , thereby improving the read stability. Moreover, the improvement primarily comes from the use of higher Vt NMOS transistors. Hence, improvement in stability from *HighVtN* to *AllHVT* is not very significant (Fig. 12).

B. Write-Ability With High Vt

As explained in Section III-A, use of high Vt transistors increases the trip point of the inverter P_R-N_R , thereby helping to improve the write-ability (see (3)). Using high Vt NMOS (S_L) reduces the discharging current (degrading write-ability) but using high Vt PMOS transistor (P_L) increases the discharging current for node 'L' (improving write-ability). Hence, it can be concluded that, migrating from *AllNomVt* to *HighVtN* does not improve the write-ability. However, use of *AllHVT* cell improves the write-ability (Fig. 13). A larger improvement is achieved at higher variation of the process parameters.

IV. STABILITY WITH THICK-OXIDE TRANSISTORS

The use of high-Vt transistors in a cell reduces the subthreshold leakage of an SRAM cell. However, in nano-scale transistors gate leakage is a major contributor to the total leakage. Hence, to reduce the total leakage of the cell it is necessary to reduce the gate leakage of the cell transistors. Fig. 1 shows the different transistors that contribute to the gate leakage. Fig. 14(a) shows the different leakage component of an SRAM cell for different Vt and Tox assignment (ThickN1.5 \equiv High Vt & Thick Oxide (by 1.5 Å°) NMOS and Nominal Vt Nominal Oxide PMOS; ThickN1.5HvtP \equiv High Vt & Thick Oxide (by 1.5 Å°) NMOS and High Vt Nominal oxide PMOS; ThickN3.0HvtP \equiv High Vt & Thick Oxide (by 3 Å°) NMOS and High Vt Nominal oxide PMOS). It can be observed that, use of AllHighVt cell reduces the subthreshold leakage of the cell. However, in AllHighVt cell gate leakage is the dominant leakage mechanism (at T = 25 C). Hence, using thick oxide NMOS devices significantly reduces the total leakage from the AllHighVt case. It should be noted that, thick oxide PMOS does not have a strong impact as the gate leakage in PMOS is much lower than that in NMOS. It can be noted that, use of thick oxide NMOS and all high Vt devices results in 11X reduction in total cell leakage compared to the cell with all nominal Vt and all nominal Tox. The improvement increases at a higher temperature. The performance degradation associated with the 11X leakage reduction from AllNomVt to ThickN3.0HvtP is negligible ($\sim 5\%$) (Fig. 14(b)). Hence, use of thicker oxide (and higher Vt) devices is efficient in reducing cell leakage with negligible performance penalty. In the following section we will analyze the effect of thicker oxide devices on read stability and write-ability.

A. Read Stability With Thick-Oxide Devices

Increasing the oxide thickness of the NMOS transistors increases the trip point of the inverter P_L-N_L . To understand that let us consider the expression of V_{TRIP} from (5):

$$\begin{aligned}
 V_{TRIP} &= \frac{V_{DD} - V_{tp} + V_{tn0} \sqrt{\left(\frac{\beta_{NL}}{\beta_{PL}}\right)}}{1 + \sqrt{\left(\frac{\beta_{NL}}{\beta_{PL}}\right)}} \\
 &= \frac{V_{DD} - V_{tp} + V_{tn0}r}{1 + r}; \text{ where,} \\
 r &= \sqrt{\left(\frac{\beta_{NL}}{\beta_{PL}}\right)} \Rightarrow \frac{\partial V_{TRIP}}{\partial r} \\
 &= \frac{V_{tn0}(1+r) - (V_{DD} - V_{tp} + V_{tn0}r)}{(1+r)^2} \\
 &= -\frac{(V_{DD} - V_{tp} + V_{tn0})}{(1+r)^2} < 0
 \end{aligned} \tag{8}$$

Increasing the T_{ox} of the NMOS alone reduces β_{NL} thereby reducing r ($= \sqrt{\beta_{NL}/\beta_{PL}}$). Hence, from (8) it can be observed that increasing the oxide thickness of NMOS increases the trip-point thereby improving the read stability. Moreover, increasing oxide thickness of NMOS reduces the strength of

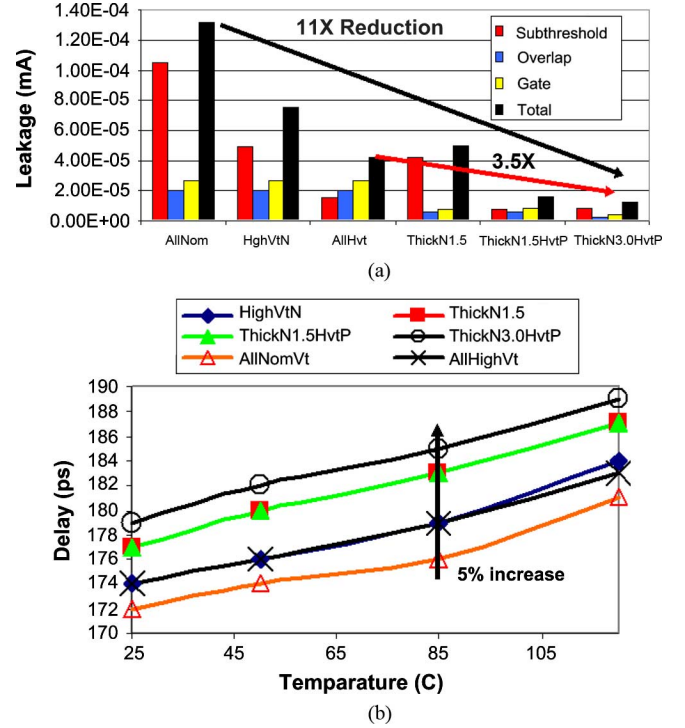


Fig. 14. Effect of Vt and oxide thickness of different devices on SRAM cell: (a) Leakage components for different Vt and T_{ox} assignment, and (b) Cell performance (read delay) for different Vt and Tox assignment.

both N_R (NMOS transistor) and S_R (access transistor). Since the access transistor has a stronger impact on read stability (see Fig. 5), increasing the NMOS oxide thickness helps to reduce NV_{READ} thereby further improving the read stability. From Fig. 15(a) use of thicker oxide NMOS devices shows a large improvement in read stability (Fig. 15(a)). First, compared to *HvtN* case increasing NMOS oxide thickness (ThickN1.5) results in a significant improvement in read stability. The similar improvement is also observed from *AllHigh* to *ThickN1.5HvtP*. However, increasing NMOS oxide thickness from 1.5 Å° to 3.0 Å° does not result in significant additional improvement. It is also interesting to note that, the minimum stable V_{DD} for ThickN1.5 is marginally higher than ThickN1.5HvtP. This is due to the fact that, a higher Vt PFET reduces the trip-point and hence degrades stability for low V_{DD} as explained in Section II.

B. Write-Ability With Thick-Oxide Devices

As explained in Section IV-A, use of thick-oxide NMOS transistors increases the trip point of the inverter P_R-N_R , thereby helping to improve the write-ability. On the other hand, higher oxide thickness of S_L reduces its strength. Consequently, the rate of discharge of node L (storing “1”) reduces. However, it should be noted that, increasing the Tox of S_L marginally improves its mobility (lower vertical electric field implies lower scattering). Hence, the overall impact in the discharge rate of node “L” is marginal ($\sim 1\%$). This is evident from the negligible (1%) increase in the write delay associated with the thick oxide cells. Hence, the overall impact of thick oxide cells on write-ability is marginal. Fig. 15(b) shows that, the write-ability of the AllHvt cell is much better compared

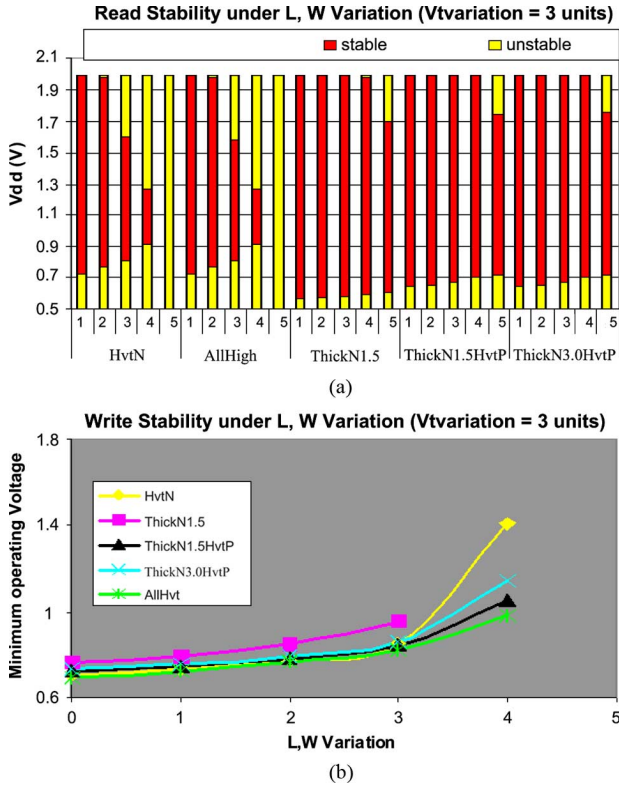


Fig. 15. Impact of using high-Vt and thick-oxide transistors on (a) Read-stability, and (b) Write-ability. X-axis represents different units L, W variations along with 3 units of Vt variations.

to the other cases. Increasing the thickness of NMOS devices with nominal Vt PMOS *ThickN1.5* significantly worsens write-ability. With a high-Vt PMOS, increasing NMOS oxide thickness results in marginal degradation of write-ability. From Figs. 15(a) and 15(b) it can be observed that, all highVt devices with thick-oxide NMOS device can result in significantly lower leakage and better read stability, with marginally lower performance and write-ability. Use of thick-oxide PMOS along with thick-oxide NMOS can result in further leakage saving and better-write-ability with a minimal impact on read stability. This is verified through hardware measurement as shown later.

V. TEST-CHIP DESIGN AND MEASUREMENT RESULTS

A test-chip is designed in sub-90nm PD/SOI technology to evaluate the effects of threshold voltage and gate oxide thickness on SRAM cell stability. The die photo for the SRAM cell stability characterization macro is shown in Fig. 16(a) and the detail layout is shown in Fig. 17(a). The designed the SRAM fly cell macro uses a 25-pad-set to characterize the dense SRAM cell device DC parametrics for a 36 Kbit SRAM array. The SRAM devices cells are wired out using metal layer. Two inverters in the cell are disconnected to accurately characterize the devices and cell stability. The device threshold voltage of each of the six transistors is measured in-line at room temperature and nominal supply voltage (1.0 V for this technology). The saturation threshold voltage (V_{tsat}) is defined by the gate-source voltage (V_{gs}) at which the drain is connected to supply voltage

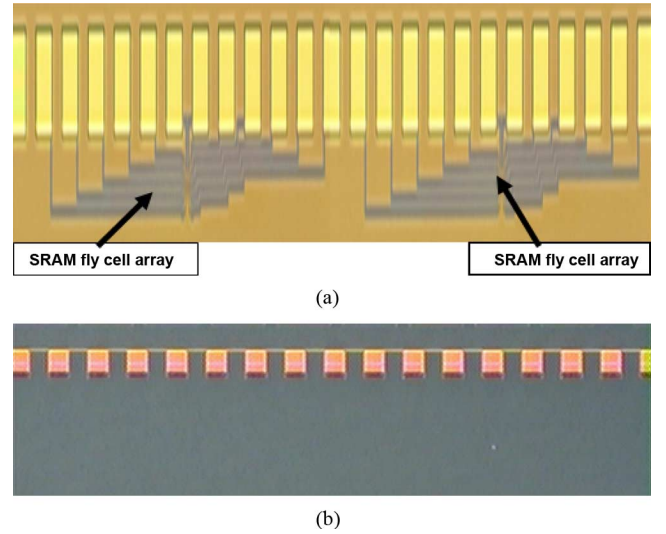


Fig. 16. Die-photo of the SRAM array showing (a) The fly cells for stability characterization, and (b) SRAM yield monitor.

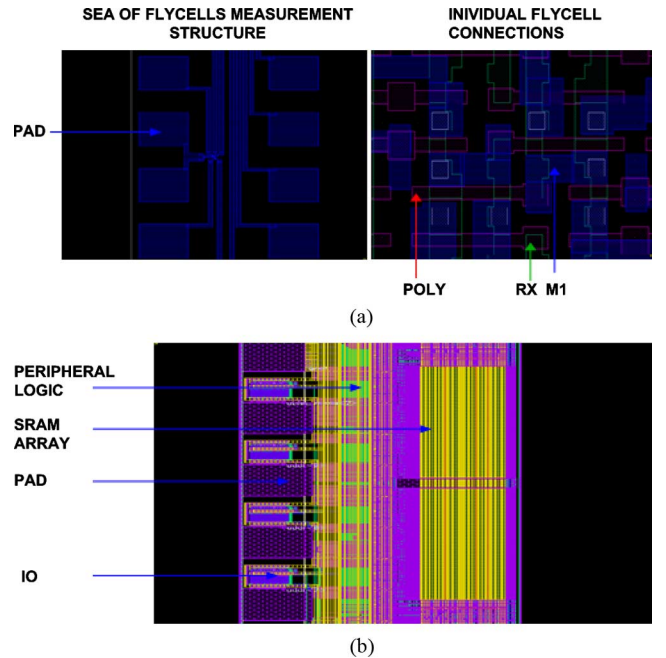


Fig. 17. Layout of the SRAM array showing (a) The fly cells for stability characterization, and (b) SRAM yield monitor (layouts are also shown as actual photomicrographs are obscured by metal fill).

and the source-drain current reaches 300 nA/um, and 70 nA/um, for N-type and P-type, respectively. The yield of SRAM is based on 1 Mbit arrays. Fig. 16(b) shows the die-photo of the SRAM yield monitor and Fig. 17(b) shows the layout. Onchip yield monitor circuits are used to measure the yield.

Fig. 18 shows the effect of device threshold voltage on read and write-ability of SRAM cells (normalized stability values are shown). The V_{th} value for all cell devices are increased in the fabricated cells. As predicted in Section III, use of higher Vt improves both read and write-ability, whether lower Vt degrades both of them. The high-Vt NMOS improves the read-stability while high-Vt PMOS results in better write-ability. Moreover,

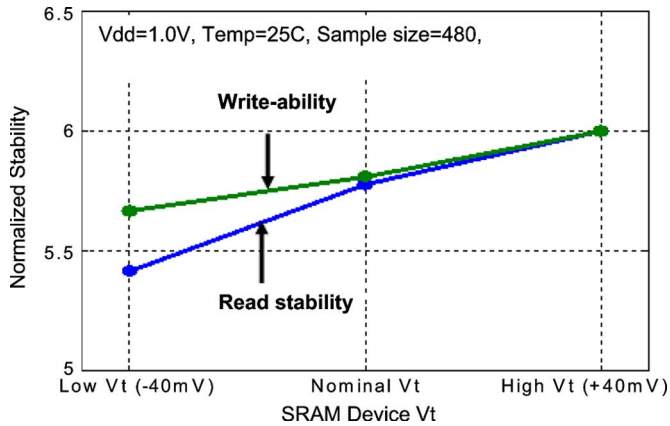


Fig. 18. Stability improvement with higher V_t devices.

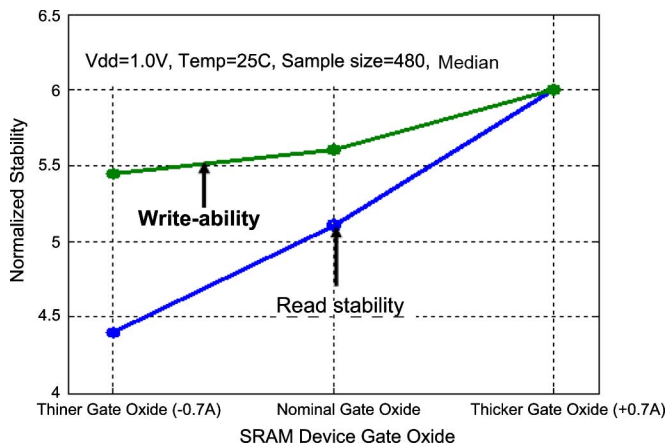


Fig. 19. Stability improvement with thicker oxide devices.

it can be observed that, the use of high- V_t improves read-stability more strongly. This is because, as explained in Section III, higher V_t simultaneously increases trip voltage and reduces read voltage. The improvement is less for write-ability. This is because, with a higher V_t the pass transistors becomes weaker and negatively impacts write-ability and reduces the overall improvement of write-ability. Fig. 19 shows the effects of oxide thickness on read and write-ability. The oxide-thickness for both NMOS and PMOS are increased in the fabricated cells. As predicted in Section IV, use of thicker oxide NMOS improves read-stability and thicker-oxide PMOS improves write-ability. Therefore, thicker-oxide cells have both read stability and write-ability. Further, improvement of read stability is more compared to the write-ability. Fig. 20 shows the yield improvement of a 1Mbit array with the use of higher V_t pass gate devices. It can be observed that, significant yield improvement can be achieved with the use of higher V_t . Further, this shows that proper design/optimization of the device V_t may be helpful for yield improvement.

VI. CONCLUSIONS

With increasing variation in the process parameters, the dynamic stability of the SRAM cell during read and write

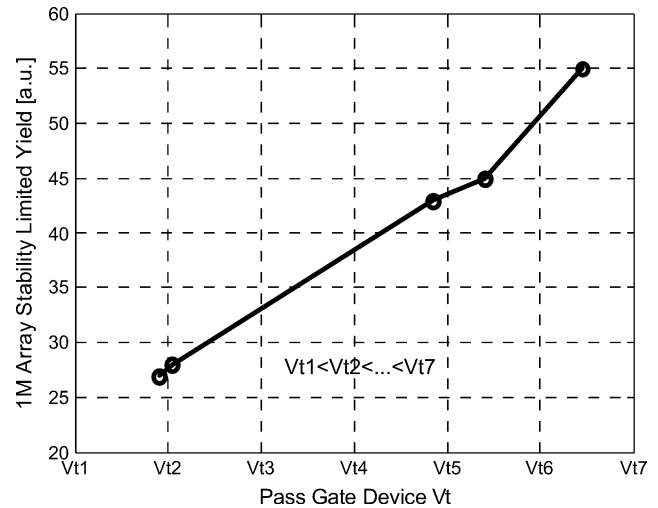


Fig. 20. Yield improvement with optimization of V_t value of higher- V_t devices.

operations has emerged as a serious design challenge. In this work we have presented a detailed study of the read and the write-ability for a sub-100 nm PD/SOI SRAM cell under parameter variations. PD/SOI specific aspects such as floating body effect and gate-to-body tunneling current were considered. The floating body effect was shown to degrade the read stability while improving the write-ability. On the other hand, the gate-to-body tunneling current improved the read stability while degrading the write-ability. The impact of using high V_t and thick oxide transistors in the cell on the cell stability has been evaluated and it has been shown that, high V_t and thick oxide cells offer improvement in leakage, read and write-ability without causing significant performance degradation. The study provided the basic understanding for maintaining/exploiting PD/SOI SRAM performance advantage and is corroborated with the SRAM hardware data.

REFERENCES

- [1] V. De *et al.*, "Technology and design challenges for low power and high performance," in *Proc. ISLPED*, 1999, pp. 163–168.
- [2] R. V. Joshi *et al.*, "Variability analysis for sub-100 nm PD/SOI SRAM cell," in *Proc. European Solid State Circuit Conf.*, Sep. 2004, pp. 211–214.
- [3] A. J. Bhavnagarwala *et al.*, "The impact of intrinsic device fluctuations on CMOS SRAM cell stability," *IEEE J. Solid-State Circuits*, vol. 36, no. 4, pp. 658–665, Apr. 2001.
- [4] R. V. Joshi *et al.*, "High performance SRAMs in 1.5 V 0.18 μm partially depleted SOI technology," in *Symp. VLSI Circuits Dig.*, 2002, pp. 74–77.
- [5] A. Chandrakasan *et al.*, *Design of High-Performance Microprocessor Circuits*. Piscataway, NJ: IEEE, 2001, ch. 14.
- [6] R. V. Joshi *et al.*, "Effects of gate-to-body tunneling current on PD/SOI CMOS SRAM," in *Symp. VLSI Technology Dig.*, 2001, pp. 75–76.
- [7] R. V. Joshi *et al.*, "Statistical exploration of the dual supply voltage space of a 65 nm PD/SOI CMOS SRAM cell," in *Proc. European Solid State Circuit Conf.*, Sep. 2006, pp. 315–318.
- [8] S. Mukhopadhyay *et al.*, "Modeling of failure probability and statistical design of SRAM array for yield enhancement in nanoscaled CMOS," *IEEE Trans. CAD*, vol. 24, no. 12, pp. 1859–1880, Dec. 2005.
- [9] A. Bansal *et al.*, "Device-optimization technique for robust and low-power FinFET SRAM design in nanoscale era," *IEEE Trans. Electron Devices*, vol. 54, no. 6, pp. 1409–1419, Jun. 2007.



Rajiv V. Joshi received the B.Tech. degree from the Indian Institute of Technology, Bombay, India, the M.S. degree from the Massachusetts Institute of Technology (MIT), and the Doctorate in Engineering Science from Columbia University, New York.

He is a Research Staff Member at IBM T. J. Watson Research Center. He joined IBM in Nov 1983, and worked on VLSI Technology (NMOS, and CMOS, sub-0.5 μm CMOS logic, DRAM and SRAM technologies). He developed novel interconnect processes and structures for Aluminum,

tungsten and Copper technologies which are widely used in IBM for various sub-0.5 μm memory and logic technologies as well as across the globe. His circuit and CAD work is used in IBM main frame and power PC processors.

Dr. Joshi has received three Corporate and two Outstanding Technical Achievement Awards from IBM. He also received 48 Invention Plateau awards from IBM. He has authored or coauthored over 140 research papers and presented several invited and keynote talks and tutorials in IEEE SOI, SSDM, ICCAD, CICC, ASYNC, AMC, and coauthored tutorials in ISSCC and DAC. He holds 130 U.S. patents in addition to several pending patents. He received the Lewis Winner Award in 1992 for an outstanding paper he coauthored at the IEEE International Solid-State Circuit Conference. He is an IEEE fellow and ISQED fellow. He received the Distinguished Alumnus Award in 2008 from IIT, Bombay. He is in program committees of IEEE ISLPED, IEEE VLSI Design, IEEE International SOI Conference (2000–2003), and ISQED. He was a general chair for 2004 ISLPED.



Saibal Mukhopadhyay (S'99–M'07) received the B.E. degree in electronics and telecommunication engineering from Jadavpur University, Calcutta, India, in 2000. He received the Ph.D. degree in electrical and computer engineering from Purdue University, West Lafayette, IN, in 2006.

He is with the School of Electrical and Computer Engineering at Georgia Institute of Technology, Atlanta, GA, as an Assistant Professor. Prior to joining Georgia Tech, he was with the IBM T. J. Watson Research Center, Yorktown Heights, NY, as a Research

Staff Member and worked on high-performance circuit design and technology-circuit co-design focusing primarily on static random access memories. His research interests include analysis and design of low-power and robust circuits in nanometer technologies.

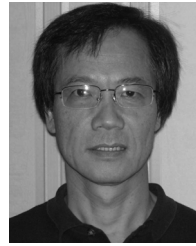
Dr. Mukhopadhyay received the IBM Ph.D. Fellowship Award for 2004–2005. He received the SRC Technical Excellence Award in 2005, the Best in Session Award at the 2005 SRC TECNCON, and Best Paper Awards at 2003 IEEE Nano and the 2004 International Conference on Computer Design. He has authored or coauthored more than 50 papers in refereed journals and conferences.



Donald W. Plass received the B.S. degree in electrical engineering from Union College in 1980.

He is a Distinguished Engineer in the IBM Systems and Technology Group. He has been responsible for SRAM technology and designs for several generations of IBM server designs, including I, P, and Z-series microprocessors, with a focus on the larger arrays. He joined IBM in 1978 at the Poughkeepsie facility. In addition to CMOS SRAM, his research and development interests have included DRAM, GaAs, and BiCMOS. He has received numerous awards for

his contributions to POWER4, POWER5, and S/390 microprocessors, and holds 27 U.S. patents.



Yuen H. Chan (M'??) received the B.S. degree in electrical engineering from Union College in 1977 and the M.S.E.E. from Syracuse University, Syracuse, NY, in 1984.

He is a Senior Technical Staff Member at the IBM Poughkeepsie Development Laboratory, working on custom VLSI circuit and SRAM designs. He joined IBM at the East Fishkill facility in 1977, and has worked on high performance Bipolar, BiCMOS, and CMOS logic and array development. He is currently a technical lead of the IBM Server Group's array design

team, supporting both the zSeries and pSeries microprocessor applications.

Mr. Chan received an IBM Corporate Award for S/390 CMOS High Frequency Techniques, and several IBM Outstanding Technical Achievement and Outstanding Innovation Awards for high performance array development. He has authored or coauthored many technical papers in the IEEE circuit conferences, the *IBM Journal of Research and Development*, and the *IBM Technical Publication Bulletin*. He is a "Master Inventor" in the IBM Poughkeepsie site. He has reached the 16th IBM Invention Achievement Plateau and holds over 40 circuit patents.



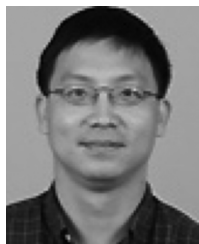
Ching-Te Chuang (S'78–M'82–SM'91–F'94) received the B.S.E.E. degree from National Taiwan University, Taipei, Taiwan, in 1975 and the Ph.D. degree in electrical engineering from the University of California, Berkeley, in 1982.

From 1977 to 1982, he was a research assistant in the Electronics Research Laboratory, University of California, Berkeley, working on bulk and surface acoustic wave devices. He joined the IBM T. J. Watson Research Center, Yorktown Heights, NY, in 1982. From 1982 to 1986, he worked on scaled

bipolar devices, technology, and circuits. He studied the scaling properties of epitaxial Schottky barrier diodes, did pioneering works on the perimeter effects of advanced double-poly self-aligned bipolar transistors, and designed the first sub-nanosecond 5 Kb bipolar ECL SRAM. From 1986 to 1988, he was Manager of the Bipolar VLSI Design Group, working on low-power bipolar circuits, high-speed high-density bipolar SRAMs, multi-Gb/s fiber-optic data-link circuits, and scaling issues for bipolar/BiCMOS devices and circuits. Since 1988, he has managed the High Performance Circuit Group, investigating high-performance logic and memory circuits. Since 1993, his group has been primarily responsible for the circuit design of IBM's high-performance CMOS microprocessors for enterprise servers, PowerPC workstations, and game/media processors. Since 1996, he has been leading the efforts in evaluating and exploring scaled/emerging technologies, such as PD/SOI, UT/SOI, strained-Si devices, hybrid orientation technology, and multi-gate/FinFET devices, for high-performance logic and SRAM applications. Since 1998, he has been responsible for the Research VLSI Technology Circuit Co-design strategy and execution. His group has also been very active and visible in leakage/variation/degradation tolerant circuit and SRAM design techniques.

Dr. Chuang has received an Outstanding Technical Achievement Award, a Research Division Outstanding Contribution Award, five Research Division Awards, and 12 Invention Achievement Awards from IBM. He took early retirement from IBM to join National Chiao-Tung University, Hsinchu, Taiwan, as a Chair Professor in the Department of Electronic Engineering in February 2008. He has received the Outstanding Scholar Award from Taiwan's Foundation for the Advancement of Outstanding Scholarship for 2008 to 2013.

Dr. Chuang served on the Device Technology Program Committee for IEDM in 1986 and 1987, and the Program Committee for Symposium on VLSI Circuits from 1992 to 2006. He was the Publication/Publicity Chairman for Symposium on VLSI Technology and Symposium on VLSI Circuits in 1993 and 1994, and the Best Student Paper Award Sub-Committee Chairman for Symposium on VLSI Circuits from 2004 to 2006. He was elected an IEEE Fellow in 1994 "for contributions to high-performance bipolar devices, circuits, and technology". He has authored many invited papers in international journals including *International Journal of High Speed Electronics*, *Proceedings of the IEEE*, *IEEE Circuits and Devices Magazine*, and *Microelectronics Journal*. He has presented numerous plenary, invited or tutorial papers/talks at international conferences such as International SOI Conference, DAC, VLSI-TSA, ISSCC Microprocessor Design Workshop, VLSI Circuit Symposium Short Course, ISQED, ICCAD, APMC, VLSI-DAT, ISCAS, MTTDT, and WSEAS. He was a corecipient of the Best Paper Award at the 2000 IEEE International SOI Conference. He holds 27 U.S. patents with 14 pending. He has authored or coauthored over 260 papers.



Yue Tan received the B.S. and M.S. degrees in electronic engineering from Southeast University, China, in 1991 and 1995, respectively, and the Ph.D. degree in electrical and electronic engineering from the Hong Kong University of Science and Technology (HKUST), where he designed and implemented a fully integrated SOI RF power amplifier for 900 MHz wireless applications. Meanwhile, he also developed a high voltage (100 V) CMOS technology for Plasma Display Panel application in a $0.6\ \mu\text{m}$ technology.

In 2001, he joined IBM Microelectronics Division. He began work on SOI RF devices and integrated circuits design at IBM Semiconductor Research and Development Center in Hopewell Junction, NY, as a

means of supporting early SOI device, technology, and electronic design automation learning for foundry business and product in 130 nm and 90 nm technology nodes. Since 2003, he has applied his interest in developing traditional 6-T SRAM for leading-edge technologies for bulk and SOI. Currently, Dr. Tan is taking SRAM cell ownership responsibility for IBM SOI technology. He is developing the highest performance SRAM cell for a given area with robust manufacturing process window and optimized for product yield and minimum array operating voltage from 90 nm to 22 nm technology nodes. Focusing predominantly on SOI device, circuit design, electronic design automation, and technology integration, He has authored or coauthored more than 30 papers in technical journals and referred conferences. He holds many published and pending U.S. patents.